REPORT DOCUMENTATION PAGE

Form Approved OMB NO. 0704-0188

1. AGENCY USE ONLY (Leave Blank)	2. REPORT DATE:	3. REPORT TYPE AND DATES COVERED Final Report 10-May-2004 - 8-Oct-2005

4. TITLE AND SUBTITLE
Electronic Sensing for Microfluidic Devices

5. FUNDING NUMBERS
W911NF0410189

6. AUTHORS
Lydia L. Sohn, David Beebe, and Daniel Notterman

8. PERFORMING ORGANIZATION REPORT NUMBER

7. PERFORMING ORGANIZATION NAMES AND ADDRESSES
University of California - Berkeley
Sponsored Projects Office
336 Sproul Hall #5940
Berkeley, CA 94720 -5940

9. SPONSORING/MONITORING AGENCY NAME(S) AND ADDRESS(ES)
U.S. Army Research Office
P.O. Box 12211
Research Triangle Park, NC 27709-2211

10. SPONSORING / MONITORING AGENCY REPORT NUMBER
45695-LS-DRP.1

11. SUPPLEMENTARY NOTES
The views, opinions and/or findings contained in this report are those of the author(s) and should not contrued as an official Department of the Army position, policy or decision, unless so designated by other documentation.

12. DISTRIBUTION AVAILIBILITY STATEMENT
Approved for Public Release; Distribution Unlimited

12b. DISTRIBUTION CODE

13. ABSTRACT (Maximum 200 words)
The abstract is below since many authors do not follow the 200 word limit

14. SUBJECT TERMS
microfluidics, electronic detection, cells

15. NUMBER OF PAGES
Unknown due to possible attachments

16. PRICE CODE

17. SECURITY CLASSIFICATION OF REPORT	18. SECURITY CLASSIFICATION ON THIS PAGE	19. SECURITY CLASSIFICATION OF ABSTRACT	20. LIMITATION OF ABSTRACT
UNCLASSIFIED	UNCLASSIFIED	UNCLASSIFIED	UL

Report Title

Electronic Sensing for Microfluidic Devices: Final Report

ABSTRACT

Rapid characterization of biological specimens is increasingly important in research and clinical applications. While current optical and chemical detection techniques can effectively analyze biological systems, a number of disadvantages restrict their versatility. As examples: most samples require advanced processing such as PCR amplification or chemical treatment, and photobleaching often limits the optically probing of fluorophore-tagged samples. Purely electronic techniques, such as those we propose here, provide solutions to many such problems, as they can probe a sample directly without requiring special modification. Equally important, readout is direct and, consequently, sensors can be easily integrated with electronics, making the entire system compact and robust. We developed a series of integrated microfluidics devices that are capable of detecting DNA in cells and the cell-surface expression of proteins on the cell-surface walls. As well, we developed an integrated microfludiics chip that is capable of performing simultaneous measurement of several sensors.

List of papers submitted or published that acknowledge ARO support during this reporting period. List the papers, including journal references, in the following categories:

(a) Papers published in peer-reviewed journals (N/A for none)

A. Carbonaro and L. L. Sohn, A Resistive Pulse Sensor for Multianalyte Detection, Lab Chip 5, 1155-1160 (2005).

Number of Papers published in peer-reviewed journals: 1.00

(b) Papers published in non-peer-reviewed journals or in conference proceedings (N/A for none)

1. S. W. Mohanty, L. L. Sohn, and D. J. Beebe, Hybrid Polymer/Thin-Film Impedance System for Label-Free Monitoring of Cells, 26th Annual International Conference, IEEE Engineering in Medicine and Biology Society, 2004.

2. O. A. Saleh and L. L. Sohn, Biological Sensing with an On-Chip Resistive Pulse Analyzer, 26th Annual International Conference, IEEE Engineering in Medicine and Biology Society, 2004.

3. I. H. Chan, A. Carbonaro, and L. L. Sohn, Artificial Pores for Performing Immunoassays, to appear in the International Conference on Miniaturized Chemical and Biochemical Analysis Systems 2004, Kluwer Academic Publishers (2004).

Number of Papers published in non peer-reviewed journals: 3.00

(c) Papers presented at meetings, but not published in conference proceedings (N/A for none)

Number of Papers not Published: 0.00

(d) Manuscripts

Number of Manuscripts: 0.00

Number of Inventions:

Graduate Students

NAME	PERCENT_SUPPORTED	
Andrea Carbonaro	1.00	No
Swomitra K. Mohanty	0.50	No
FTE Equivalent:	**1.50**	
Total Number:	**2**	

Names of Post Doctorates

NAME	PERCENT_SUPPORTED	
Ian Chan	1.00	No
FTE Equivalent:	**1.00**	
Total Number:	**1**	

Names of Faculty Supported

NAME	PERCENT_SUPPORTED	National Academy Member
Lydia L. Sohn	0.10	No
David Beebe	0.10	No
Daniel Notterman	0.00	No
FTE Equivalent:	**0.20**	
Total Number:	**3**	

Names of Under Graduate students supported

NAME	PERCENT_SUPPORTED	
N.A.		No
FTE Equivalent:		
Total Number:	**1**	

Names of Personnel receiving masters degrees

NAME		
N.A.	No	
Total Number:	**1**	

Names of personnel receiving PHDs

NAME		
N.A.	No	
Total Number:	**1**	

Names of other research staff

NAME	PERCENT_SUPPORTED
FTE Equivalent:	
Total Number:	

Sub Contractors (DD882)

1 a. University of Wisconsin-Madison

1 b. 2142 Engineering Centers Building
1550 Engineering Drive
Madison WI 53706

Sub Contractor Numbers (c): SA4403-32439
Patent Clause Number (d-1):
Patent Date (d-2):
Work Description (e): David Beebe (Dept. of Bioengineering) fabricated the microfluidic devices using uFT. H
Sub Contract Award Date (f-1): 5/10/2004 12:00:00AM
Sub Contract Est Completion Date(f-2): 10/8/2005 12:00:00AM

---

1 a. Robert Wood Johnson Medical School

1 b. 675 Hoes Lane, Room 705

Piscataway N.J. 088545635

Sub Contractor Numbers (c): SA4404-32439
Patent Clause Number (d-1):
Patent Date (d-2):
Work Description (e): Daniel Notterman (Dept. of Pediatrics) provided guidance on sample choice and cell sam
Sub Contract Award Date (f-1): 5/10/2004 12:00:00AM
Sub Contract Est Completion Date(f-2): 10/8/2004 12:00:00AM

---

1 a. Robert Wood Johnson Medical School

1 b. 675 Hoes Lane

Piscataway NJ 08854

Sub Contractor Numbers (c): SA4404-32439
Patent Clause Number (d-1):
Patent Date (d-2):
Work Description (e): Daniel Notterman (Dept. of Pediatrics) provided guidance on sample choice and cell sam
Sub Contract Award Date (f-1): 5/10/2004 12:00:00AM
Sub Contract Est Completion Date(f-2): 10/8/2004 12:00:00AM

Inventions (DD882)

I. Statement of Problem Studied

The original goal of this ARO/DARPA-funded project was to develop a fully-integrated microfluidic device that would be capable of electronically detecting specific bacterial pathogens in whole blood and in other fluids such as sputum and urine. The integrated device proposed was to consist of two sensors on a single-chip platform: a microscale Coulter counter that would size and then fractionate blood samples based on particulate size; and an on-chip high-frequency spectrometer that would interrogate the dielectric response of an unknown pathogen (bacterial, protozoa, or yeast) at specific frequencies. By creating a library of frequencies corresponding to known cell types, we would be able to map the spectral response of an unknown organism, thus permitting very rapid identification of species and form (i.e. vegetative vs. spore).

For this final period of funding, **Lydia L. Sohn** (PI and Associate Professor of Mechanical Engineering, University of California, Berkeley), **Daniel Notterman** (co-PI and Professor in the Dept. of Pediatrics, Robert Wood Johnson Medical School), and **David Beebe** (co-PI and Professor of Bioengineering, University of Wisconsin, Madison) focused on 1) multiplexing the microscale Coulter counter such that *N* x *N* Coulter counters could operate *simultaneously*; and 2) utilizing microfluidic tectonics (μFT) instead of MEMS technology to fabricate the high-frequency spectrometer. Using μFT to fabricate our devices would ultimately allow us to integrate the two different sensors onto a single chip.

II. Summary of the Most Important Results

Multiplexing the Microscale Coulter Counter

Detecting specific antigens in human serum is a necessary step to diagnose, monitor, and understand a potential illness. In certain cases, only a combination of different immunoassays can reveal the presence of a pathologic condition. Current multianalyte techniques are based on the long-established sandwich immunoassay in which a capture antibody is used to immobilize a specific antigen on the assay surface and a chemically- or biologically-labeled detection antibody is used to mark the presence of the antigen. Multianalyte techniques, however, differ from traditional sandwich immunoassays in their need for separate test zones—one per each particular antigen—and for the use of two or more labels (one per analyte).[1,2] Just as conventional sandwich immunoassays have a number of drawbacks, including lengthy incubation times for functionalizing the assay surface with the capture antibodies (typically 15 hours[3]) and the need to label the detection antibodies (which incurs additional steps and reagent use), current multianalyte detection schemes have drawbacks as well. For example only fluorescent labels having different emission wavelengths or kinetics can be employed; as another example, multiple incubation steps are often required. Clearly, there is a compelling need to develop new methods for sensing multiple antigens simultaneously.

In this project, we demonstrated, for the first time, the ability to perform multianalyte immunoassays using multiple artificial pores (i.e. microscale Coulter counters) on a single chip.[4] Previously, we had shown that our pore is highly effective in circumventing the drawbacks of traditional sandwich immunoassays[5,6]: incubation times are significantly reduced and labeling is not necessary because the technique is purely electronic and therefore label-free and direct. Here, we showed that resistive-pulse sensing could be used to detect simultaneously two different human antigens on a single chip. Specifically, we demonstrated that we could detect concurrently human granulocyte and macrophage colony stimulating factor (GM-CSF) and granulocyte colony stimulating factor (G-CSF), both of which are associated with acute inflammation [8] and can be involved with tumor progression.[7,8] While we chose GM-CSF and G-CSF detection as our proof-of-principle, we emphasize that our pore technique can be

applied to a wide variety of ligands that can be detected simultaneously, thus making this technique a key platform technology for multiple immunoassays.

Using standard microfabrication and soft-lithography techniques, we fabricated two 10 µm x 1µm x 1 µm (L x W x H) pores on a single chip (Figure 1). The assay colloids used in these experiments were 490 nm streptavidin-coated colloids from Bangs Labs (Fishers, IN), and the reference colloids used to calibrate the pores were 470 nm sulfate-coated polystyrene colloids from Interfacial Dynamics (Portland, OR). While the assay colloids were diluted to a working concentration of 1.4×109 colloids/mL (1:100 dilution), the reference colloids were diluted to 1.2×109 colloids/mL (1:1000 dilution). The two different colloids were subsequently mixed in a buffer solution consisting of 0.5× phosphate buffered saline, 1 mg/mL bovine serum albumin (as a blocking agent), and 0.1% (v/v) Tween 20 (as a surfactant). Prior to use, both colloids were washed in buffer by centrifugation (7 krcf for 14 minutes, repeated a total of three times).

Multianalyte assays were performed simultaneously for human GM-CSF and human G-CSF antigens. The capture and unlabeled detection antibodies, as well as the reference antigens for both assays, were obtained from ELISA DuoSet kits (R&D Systems, Minneapolis, MN). To detect the antigens, the assay colloids were incubated with 10 µg/mL capture antibodies for 15 minutes to thus functionalize them. The colloids are then thoroughly washed to remove the excess antibodies from solution. The assay colloids conjugated to primary antibodies were injected into the dual pore device connected to the electronic apparatus described above and an external pressure (1-3 psi) is applied to drive the colloids through each pore. The change in resistance due to a colloid passing through the

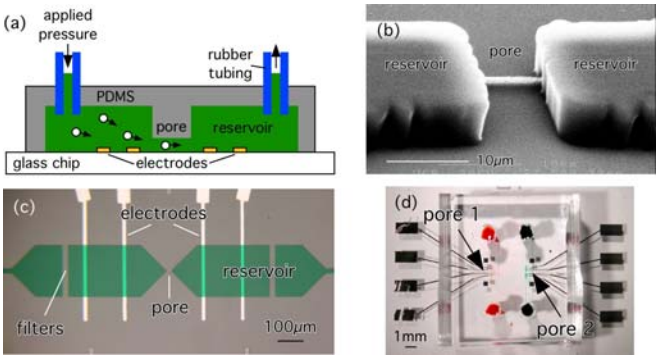

Figure 1: Design of resistive-pulse sensor. (a) Side-view schematic of a single pore. A molded PDMS slab containing the reservoirs and pore is sealed to a glass chip with prefabricated Ti/Pt electrodes. (b) SEM picture of master mold highlighting details of the pore and reservoirs. (c) Optical view of completed sensor as viewed from the top. Microfluidic channels have been filled with dye for enhanced visibility. (d) Photograph of dual pore sensor containing two separate pores on a single chip.

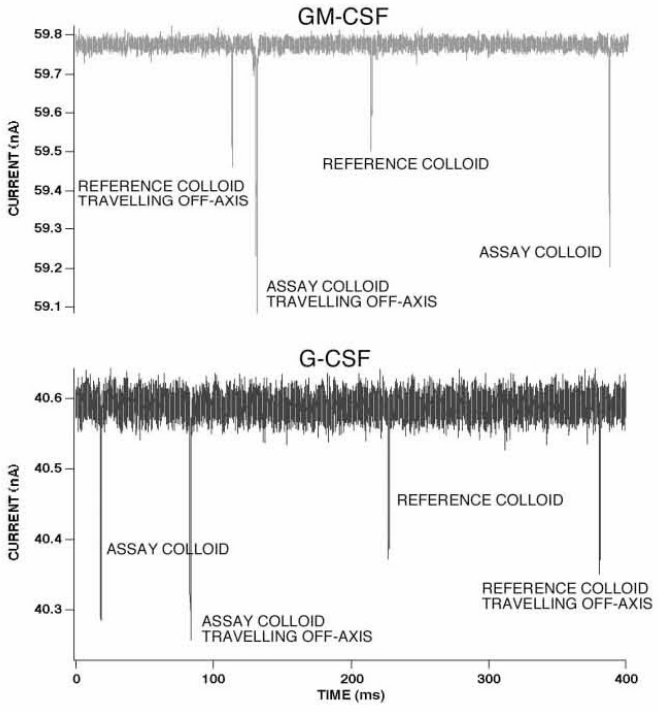

Figure 2: Representative data from Pore 1 and Pore 2 measured simultaneously in the dual pore sensor. Each pulse in the data corresponds to a single colloid. Pore 1 was used to assay GM-CSF antigens while Pore 2 was used to assay G-CSF antigens.

pore was measured and the following relationship was used to used to determine the mean colloid diameter [5,6,9]:

$$\frac{dI}{I} = \frac{d^3}{LD^2}\left[\frac{D^2}{2L^2} + \frac{1}{\sqrt{1+(D/L)^2}}F\left(\frac{d^3}{D^3}\right)\right] \quad (1)$$

where dI/I is the normalized current measured when a particle of size d passes through a pore of diameter D and length L, and F(d3/D3) is a numerical correction factor given as a table of values by Debois and Bean.[10] The same functionalized assay colloids were then incubated with both the antigens and detection antibodies for 20 minutes to complete the sandwich assay and the same measurements were repeated. Size changes corresponding to bound GM-CSF and human G-CSF antigens were thus detected.

Figure 2 shows representative data measured simultaneously in Pores 1 and 2 of a dual-pore device. Each pulse in the current trace corresponds to a single functionalized colloid passing through a pore. We used Pore 1 to perform an immunoassay of human GM-CSF antigens, and Pore 2 for human G-CSF. The results of several of these simultaneous immunoassays are shown in Figure 3. The data in columns B–D corresponds to the result of two measurements performed in parallel. The data in column A corresponds to the diameter of the unfunctionalized assay colloid (512.2 nm). The presence of different components in each measurement is indicated by a checkmark under each bar.

Column B shows the diameters of assay colloids after functionalizing them with human GM-CSF (left) and G-CSF (right) primary antibodies. The colloids were incubated with a buffer solution containing 10 µg/mL of biotinylated primary antibodies. With this working concentration, assay

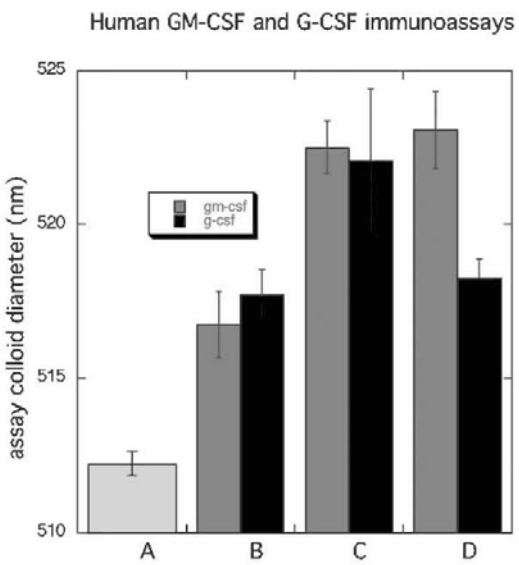

assay colloid	√	√	√	√	√	√	√
GM-CSF pri ab		√		√		√	
G-CSF pri ab			√		√		√
GM-CSF antigen				√		√	√
G-CSF antigen					√		
GM-CSF sec ab				√		√	
G-CSF sec ab					√		√

Figure 3: Mean assay colloid diameter measured under a variety of conditions. In column A, the diameter of the unfunctionalized assay colloid is indicated. In each of columns B–D, two separate but simultaneous immunoassays were conducted, one for GM-CSF antigen and the other for G-CSF antigen. In column B, the diameters of assay colloids functionalized with GM-CSF and G-CSF primary antibodies are shown. Both measurements showed clear increases in diameter of 5 nm as compared to the unfunctionalized assay colloid. In column C, immunoassays of GM-CSF and G-CSF antigens were completed, resulting in a further 5 nm increase in the diameter. This indicates that both assays detected the presence of their respective antigen. In column D, GM-CSF antigen were used in both assays, resulting in a diameter increase (compared to column B) in the GM-CSF assay, but not in the G-CSF assay. This shows that specific binding between antigen and antibodies is required for the size increase and antigen detection.

colloids in both cases showed a size increase of 5 nm over the plain assay colloids (column A).

In column C, sandwich assays for GM-CSF (left) and G-CSF (right) were completed. As indicated, the diameter of both sets of assay colloids increased by 5 nm over the functionalized colloids (column B) to 522 nm. This demonstrates that both assays positively detected the presence of their respective antigens (GM-CSF at 84 ng/mL and G-CSF at 90 ng/mL). The 5-nm diameter increase here suggests that as many secondary antibodies as primary antibodies became attached to the colloid. The volume added by the antigens is not expected to contribute significantly to the diameter increase, as the antigen is about 10× less massive than the antibody.

In the final column, column D, a control experiment was performed in which GM-CSF antigen (84 ng/mL) was added to the GM-CSF sandwich assay (left), but non-specific GM-CSF antigen (84 ng/mL) was added to the G-CSF sandwich assay (right). The assay for GM-CSF showed a clear size increase of 5 nm over the functionalized assay colloids (column B), but the assay for G-CSF did not. This shows that size increase of colloids is measured only if specific antigen-antibody binding occurs. If this condition is not satisfied antigens are not sensed.

The antigen concentrations detected were 84 ng/mL and 90 ng/mL for GM-CSF and G-CSF, respectively. Since the standard deviation of the colloid diameter is 13 nm, we can achieve a resolution of 0.2% if 200 or more colloids are measured during each experiment. This corresponds to our measuring a change in diameter as small as 1 nm in a 512 nm colloid and to our detecting a concentration as little as 15 ng/mL. To further increase the sensitivity of our device, we suggest decreasing the colloid concentration or using smaller or monodisperse colloids.

Although we have performed the necessary chemistry and incubation steps outside the chip, the microfluidic platform we have used for our dual pore sensor can readily include reservoirs and mixers for a Micro Total Analysis System (μTAS). In addition, although we demonstrated the simultaneous detection of two antigens, ours is a scalable technology that can lead to the sensing of a greater number of antigens simultaneously. Since colloids with different diameter generate pulses with different magnitude, several antigens can be detected in the same pore by assigning them to colloids of different diameters. Currently we are capable of sensing up to four differently-sized colloids in a single pore.[5] Given this and what we have demonstrated in this paper, it is thus possible to perform at least 4N2 simultaneous assays on a single chip of N x N arrays of pores. This level of multiple detection is truly unprecedented.

MicroFluidic Tectonics (μFT) for Impedance Measurements

Current methods for real-time/label free single cell monitoring include patch clamping, carbon fiber electrodes,[11] microelectrode arrays for electrical monitoring,[12] and nanoprobes for local cell area monitoring.[13] While these techniques are important, they are either invasive (e.g. patch clamp) or capable of only measuring substances outside the cell. In addition, they require careful experimental set-up, making high throughput processing difficult. Clearly new techniques are needed to expand what can be detected, most importantly, changes inside the cell. In addition these techniques should be implemented in the simplest manner possible to make them widely available. Thus inexpensive and easy fabrication techniques are important for impedance measurement devices.

Capacitive cytometry,[14] and more broadly impedance measurements, has the potential to be one important technique for live cell analysis. This method of analysis is based on interrogating a biological sample with an electrical waveform at single or varying frequencies. Capacitance cytometry relies on measuring the AC polarization response of intercellular components while impedance measurements often involve the passage of current through the cell and the subsequent measurements of the magnitude and phase of the cells internal/external environment. Each of these measurements is influenced by the state and type of the cell involved. For example, different cells types have different concentrations of ion

channels (Na, K, Ca,) embedded in the membrane. These can change the membrane capacitance resulting in different impedance signatures. The state of the ion channel (open/closed) can also affect the impedance signature providing insight to cell behavior in relation to its environment. Previously, capacitance cytometry has been used to detect changes of DNA levels within the cell over time.[14] The ability to observe real-time monitoring of DNA levels without the use of tags is an asset to biological research as it allows researchers to observe cells in an unmodified or natural state. Impedance measurements over a spectrum, has been successfully used to distinguish between different types of cells. Ayliffe et al. showed their impedance-based measurements could distinguish between red blood cells and leukocytes[15] and Mohanty et al. showed the ability to distinguish between chromaffin cells and red blood cells.[16] They also showed preliminary results looking at ion channel activity and it's relation to impedance spectrums. Gawad et al. has used impedance measurements for leukocyte discrimination and sorting applications.[17] Recently, there has been an increased interest in the relationship between the cells microenvironment and cell proliferation.[18-22] The integration of impedance measurements with micro culture systems presents interesting possibilities in regard to providing more *in vivo* like culture conditions and a non-invasive measurement within that culture environment.

The impedance measurement systems mentioned above uses traditional MEMS techniques to fabricate the devices. This is a lengthy and expensive process. In this project, we developed the means of creating a simple impedance measurement system without using MEMS technology.

For impedance spectroscopy measurements the device shown in Figure 4 is used. As shown, the device (3 have been fabricated on a single chip) consists of pair of 100 µm-wide gold (Au) electrodes patterned using standard photolithography. The slides used were purchased precoated with 100Å of Ti and 3000Å of Au. A microfluidic channel, 50 µm wide and 125 µm high, was fabricated over the electrodes using µFluidic Tectonics technology.[23] µFluidic Tectonics utilizes liquid phase photopolymerization to create micro channel networks directly on the glass substrate avoiding etching/molding and bonding steps typically required. A schematic of the sensor region is shown in the inset. As shown, the gap between the electrodes—the sensor area—spans the microfluidic channel width. The area of this region is 50 µm x 100 µm. Our use of µTectonics to fabricate the device is extraordinarily simple and quick as compared to our previously-described method of device fabrication.[14] Through the use of commercially available metal-coated glass substrates the entire device can be fabricated in a standard lab in approximately 1.5 hours.

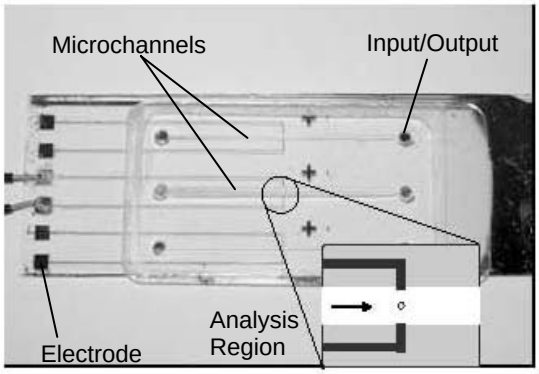

Figure 4: Microelectrical impedance spectroscopy device. Device has an array of 3 channels with opposing electrodes at the analysis region. Inset: schematic of analysis region. The cell flows down the channel and is stopped in between electrodes for analysis

We have performed initial testing of the device using air and phosphate buffer saline (PBS) solution as references. We employed an Andeen-Hagerling 2700A capacitance bridge to sweep frequency from 50 Hz to 20 kHz. Our results are shown in Figure 5—PBS clearly has a larger capacitance response as compared to air; this is expected. We next measured Fall Armyworm ovarian cells (Sf9) (cells commonly used commercially for protein production via the baculovirus system). These ovary cells were suspended in 1X Dulbecco PBS, injected in the input port, and traveled through the channel via a vacuum applied at the output port. Once a

single cell reached the sensor region (this was confirmed using an optical microscope), we removed the applied vacuum. This resulted in the cell being stationary for analysis. An appropriate time was allowed to pass in order for the cell to settle to the bottom of the microfluidic channel before measurements were taken.

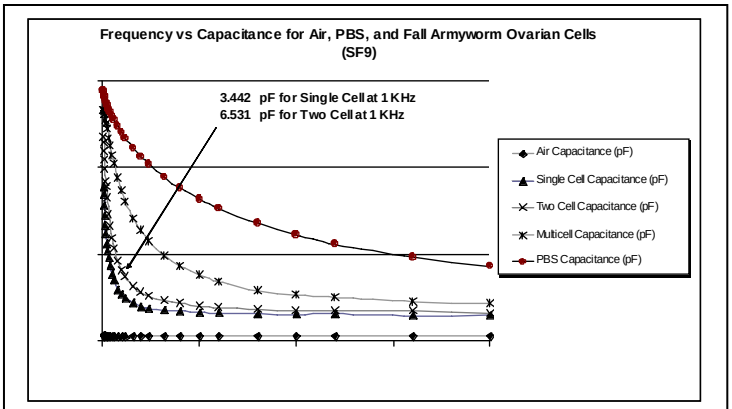

Figure 5: Frequency vs. Capacitance for Air, PBS, and Fall Armyworm cells. Air had the lowest capacitance as expected. Measurements conducted on different numbers of cells showed distinct differences at lower

Figure 5 shows the capacitance spectra of one, two, and an aggregate number of cells. The spectra clearly show the relationship between the capacitance measured and the number of cells (the lower frequencies correspond to ionic effects; the higher to DNA content of the cells). Of particular interest is the fact that at the 1 kHz frequency, the capacitance signal of two cells is nearly double that of a single cell. This is entirely consistent with our previously-published results in which capacitance cytometry showed a strong, linear relationship between the DNA content of individual cells and their dielectric (or capacitance) response to a 1 kHz field.[14]

The preliminary data in Figure 5 is very encouraging as it demonstrates the use of simple fabrication methods to create an integrated capacitance device. Such a demonstration is important as it allows for the easy incorporation of a variety of system designs and components for various applications. Ultimately, we believe capacitance cytometry/impedance spectroscopy can be used to create a database to identify a wide variety of different cell types and cell states. Thus, it may be possible to use impedance measurements to sort stem and progenitor sub-populations. Currently, cells with progenitor cell characteristics can be sorted using FACS based on observed dye exclusion. However, cells sorted by FACS are significantly degraded due to both the dye and the mechanical stress of the sorting process. Impedance measurements may provide a method for sorting cells without the associated degradation. This would be of benefit allowing further culture of healthy sorted subpopulations to explore stem/progenitor cell differentiation.

It is important to note that the effects of electric fields on cells are still an open question. Electric fields are commonly applied to cells (e.g. electroporation, dielectrophoresis) and no negative effects have been reported. However, more research is needed to determine if exposure to electric fields has any subtle effects on living cells.

While much work remains, the merging of micro culture systems with impedance-based monitoring holds much promise. The ability to monitor unique impedance signatures over time in culture without perturbing the cell could help provide both new insights into basic cell behavior as well as provide a useful tool to allow “label free” cell sorting.

III Technology Transition

During 2003-2004, the Sohn group worked with the Edgewood Chemical and Biological Center (ECBC) to train the staff scientists on how to use the micro Coulter Counter. The Sohn group fabricated and delivered ~200 devices to ECBC so that they could develop specific immunoassays that are of interest to DoD.

References

1. Bookout, J. T., Joaquim, T. R., Magin, K. M., Rogan, G. J. & Lirette, R. P. Development of a dual-label time-resolved fluorometric immunoassay for the simultaneous detection of two recombinant proteins in potato. J Agric Food Chem 48, 5868-73 (2000).
2. Eriksson, S. et al. Dual-label time-resolved immunofluorometric assay of free and total prostate-specific antigen based on recombinant Fab fragments. Clin Chem 46, 658-66 (2000).
3. Engvall, E. & Perlman, P. Enzyme-linked immunosorbent assay (ELISA). Quantitative assay of immunoglobulin G. Immunochemistry 8, 871-4 (1971).
4. Carbonaro, A. & Sohn, L. L. A resistive-pulse sensor chip for multianalyte immunoassays. Lab on a Chip 5, 1155-1160 (2005).
5. Saleh, O. A. & Sohn, L. L. Quantitative sensing of nanoscale colloids using a microchip Coulter counter. Review of Scientific Instruments 72, 4449-4451 (2001).
6. Saleh, O. A. & Sohn, L. L. Direct detection of antibody-antigen binding using an on-chip artificial pore. Proc Natl Acad Sci U S A 100, 820-4 (2003).
7. Watanabe, M. et al. Production of granulocyte-macrophage colony-stimulating factor in a patient with metastatic chest wall large cell carcinoma. Jpn J Clin Oncol 28, 559-62 (1998).
8. Kojima, K. et al. Clinicopathological study of involvement of granulocyte colony stimulating factor and granulocyte-macrophage colony stimulating factor in non-lymphohematopoietic malignant tumors accompanied by leukocytosis. Histol Histopathol 17, 1005-16 (2002).
9. Saleh, O. A. & Sohn, L. L. Correcting off-axis effects in an on-chip resistive-pulse analyzer. Review of Scientific Instruments 73, 4396-4398 (2002).
10. Deblois, R. W. & Bean, C. P. Counting and Sizing of Submicron Particles by Resistive Pulse Technique. Review of Scientific Instruments 41, 909-& (1970).
11. Chow, R. H. & von Rueden, L. Electrochemical Detection of Secretion from Single Cells (1995).
12. Gilchrist, K. H. et al. General purpose, field-portable cell-based biosensor platform. Biosens Bioelectron 16, 557-64 (2001).
13. Smith, P. J., Hammar, K., Porterfield, D. M., Sanger, R. H. & Trimarchi, J. R. Self-referencing, non-invasive, ion selective electrode for single cell detection of trans-plasma membrane calcium flux. Microsc Res Tech 46, 398-417 (1999).
14. Sohn, L. L. et al. Capacitance cytometry: measuring biological cells one by one. Proc Natl Acad Sci U S A 97, 10687-90 (2000).
15. Ayliffe, H. E., Frazier, A. B. & Rabbitt, R. D. The development of a microfabricated device to measure the electric impedance of individual leukocytes. Am. Soc. Mech. Eng. Biomedical Engineering Conference 35, 485-486 (1997).
16. Mohanty, S. K., Ravula, S. K., Engisch, K. & Frazier, A. B. A MicroAnalysis System Using Dielectrophoresis and Micro Electrical Impedance Spectroscopy for Cell Manipulation and Analysis. 12th International Conference on Solid-State Sensors, Actuators, and Microsystems (June 8-12 2003).
17. Gaward, S., Batard, P., Seger, U., Metz, S. & Renaud, P. Leukocyces Discrimmination by Impedance Spectroscopy Flow Cytometry. Micro Total Analysis Systems 2, 649-651 (2002).
18. Raty, S. et al. Embryonic development in the mouse is enhanced via microchannel culture. Lab on a Chip 4, 186-190 (2004).
19. Walker, G. M., Ozers, M. S. & Beebe, D. J. Insect cell culture in microfluidic channels. Biomedical Microdevices 4, 161-166 (2002).

20. Walker, G. M., Zeringue, H. C. & Beebe, D. J. Microenvironment design considerations for cellular scale studies. Lab on a Chip 4, 91-97 (2004).
21. Powers, M. J. et al. A microfabricated array bioreactor for perfused 3D liver culture. Biotechnol Bioeng 78, 257-69 (2002).
22. Borenstein, J. Microfabrication technology for vacularized tissue engineering. Biomedical Microdevices 4, 167-175 (2002).
23. Moorthy, J. & Beebe, D. J. Organic and biomimetic designs for microfluidic systems - New strategies offer a flexible approach to designing microscale devices. Analytical Chemistry 75, 292A-301A (2003).